

# Processing of (in)tractable polymers using reactive solvents

## Part 5: morphology control during phase separation

B.J.P. Jansen, H.E.H. Meijer\*, P.J. Lemstra

*Eindhoven Polymer Laboratories, Dutch Polymer Institute, Eindhoven University of Technology, PO Box 513, 5600 MB Eindhoven, The Netherlands*

Received 2 April 1998; accepted 4 June 1998

---

### Abstract

Processing of intractable polymers using reactive solvents (monomers) has been studied extensively in our laboratory, notably the system poly(phenylene ether) (PPE)/epoxy (resin). PPE can be dissolved at elevated temperatures in epoxy resin and the solution can be easily transferred into a mould or into a fabric. Upon curing the epoxy resin, phase separation and phase inversion occurs and the originally dissolved PPE becomes the continuous matrix phase. The dispersed (cured thermoset) epoxy particles become an integrated part of the system and could act as fillers or as toughening agents, depending on the type of epoxy resin used. An important parameter for the (ultimate) physical and mechanical properties is the size of the dispersed particles. The aim of the present study is to control the morphology development in order to produce a dispersed phase in the sub-micron to nanometre range. The size of the dispersed phase will be determined by the competition between the coarsening rate, e.g. by the coalescence of dispersed droplets, and the vitrification and/or gelation rate induced by curing. For the coarsening process, the viscosity of the system plays an important role which is usually mainly determined by the temperature. However, in the case of PPE/epoxy, the viscosity can be controlled at a chosen curing temperature by adding polystyrene. The ternary phase diagram shows that the miscibility of PPE–polystyrene (PS) is retained upon the addition of epoxy at relatively low concentrations. However, thermally induced phase separation upon cooling occurs for solutions with an epoxy content of 30 wt% and more. Upon curing, a two phase morphology is obtained in which the PPE–PS phase acts, as expected, as one single phase. The size of the dispersed phase can be decreased by one order of magnitude if curing is performed at the glass transition temperature,  $T_g$ , of the initial solution, attributed to the high viscosity at  $T_g$  that slows down coalescence. During the additional post-curing steps, necessary to reach a maximum epoxy conversion, these original morphologies are maintained. In conclusion, by controlling the polymerisation temperature, relative with reference to the  $T_g$  of the original solution, the final morphology of the chemically induced phase separated systems can be tuned. © 1999 Elsevier Science Ltd. All rights reserved.

*Keywords:* Phase separation; Morphology control; Epoxy

---

### 1. Introduction

Recently, Venderbosch et al. [1–3] introduced epoxy resin as a reactive solvent for the processing of intractable polymers such as poly(2,6-dimethyl-1,4-phenylene ether) (PPE). After processing, the homogeneous PPE–epoxy solution is cured which causes chemically induced phase separation and phase inversion, resulting in a blend of dispersed epoxy particles in a continuous PPE matrix. In contrast to the use of miscible (poly) styrene as a processing aid, the advantageous thermal (high glass transition temperature,  $T_g$ ) and mechanical properties of the PPE phase are recovered. Moreover, by using aliphatic epoxy resins, toughness enhancement was obtained by action of the final rubbery dispersed phase [3].

The solubility of PPE in epoxy resins is not unique. Many polymers can be dissolved in epoxy resins such as polystyrene, poly(methyl methacrylate) [4], polyetherimide [5,6], polysulphone [7] and polyethersulphone [8,9]. In studies concerning dissolving a thermoplastic polymer in epoxy resin, the aim was toughening of the cured thermoset epoxy matrix. In our processing route, however, the aim is that the originally dissolved thermoplast becomes the continuous matrix. The epoxy resin facilitates processing as a solvent and is ‘locked up’ after curing as useful constituent in the thermoplastic matrix.

The morphology of the cured PPE/epoxy blends will, of course, affect the final mechanical behaviour of the obtained blend. Therefore, morphology control during phase separation is of crucial importance. During physical blending of two or more immiscible polymers, the final morphology is mainly determined by the processing conditions, the

---

\* Corresponding author.

compatibility, the viscosities and viscosity ratio of the polymers involved [10]. Since in chemical blending at least one of the polymers is synthesised in the presence of the other, morphology development is even more complicated. Practical examples can be found in the fabrication of high-impact polystyrene and acrylonitrilebutadiene styrene in which styrene is (co-)polymerised in the presence of another polymer [11]. Moreover, chemical blending also includes the synthesis of an interpenetrating polymer network [12,13], in which two separate polymer networks are simultaneously polymerised. Several studies have been reported concerning the parameters which determine the final morphology in blends prepared via chemically induced phase separation [6,7,9,14–19]. Besides the intrinsic compatibility of the monomers and polymers involved, the competition between reaction kinetics and the rate of phase separation appears to be the main factor to be considered.

In this paper, the morphology control in chemically induced phase separating systems is studied using the PPE–PS/epoxy system. By changing the PPE:PS ratio, the viscosity of this system can be varied at constant curing temperature. The objective is to obtain more insight into those kinetic factors that determine the size of the final morphology, and our final interest is obtaining a sub-micron sized dispersed phase, typically 100 nm or even smaller. These morphologies can eventually be applied to improve the toughness of rubber modified brittle amorphous polymers [19].

## 2. Experimental

### 2.1. Sample preparation

PPE, PPO 803 possessing a molar mass of  $32 \text{ kg mol}^{-1}$  ( $M_w$ ), was supplied by General Electric Plastics (Bergen op Zoom, The Netherlands) and polystyrene (PS), SHELL N5000 possessing a  $M_w$  of  $260 \text{ kg mol}^{-1}$ , was supplied by BPM (Bredase Polystyreen Maatschappij, Breda, The Netherlands). As a reactive solvent for these polymers, a diglycidyl ether of bisphenol-A epoxy resin (SHELL Epikote 828 EL) was used. Two different aromatic curing agents, supplied by Lonza (Breda, The Netherlands), were used: 4,4'-methylenebis(3-chloro-2,6-diethylaniline) (M-CDEA) and 4,4'-methylenebis(2,6-diethylaniline) (M-DEA). The structural formulae of all these components have been published previously [3].

The PPE–PS blends and PPE–PS/epoxy solutions were prepared using either a Brabender Plasticorder batch kneader ( $60 \text{ cm}^3$ ) or a co-rotating miniature recirculating twin-screw extruder ( $5 \text{ cm}^3$ ). Depending on the relative content of the three constituents, a processing temperature of 150 to  $230^\circ\text{C}$  was used. Blending and dissolution was extended until a homogeneous, optically transparent, solution was obtained. High epoxy content solutions ( $>60 \text{ wt}\%$ ) of PS/

epoxy were prepared by stirring a mixture of PS and epoxy in a glass beaker at  $\pm 120^\circ\text{C}$ .

After a homogeneous solution was obtained, the curing agent, if any, was added (51 phr for M-CDEA, 43.3 phr for M-DEA), and mixing was continued for several minutes. The solutions obtained were compression moulded and, subsequently, cured at various temperatures. The exact curing temperatures and times will be indicated.

### 2.2. Solution behaviour

The phase behaviour of the binary PS/epoxy and the ternary PPE–PS/epoxy system, was studied using a light scattering set up. Compression moulded films were heated between two glass slides in a Linkham Hot Stage until a homogeneous solution was obtained. The intensity of a laser beam, which was directed through the sample, was recorded using a light detector. The reported cloud point temperatures correspond with the onset of the measured decrease in light transmission, caused by phase separation of the samples upon cooling ( $2^\circ\text{C min}^{-1}$ ). All solutions showed an upper critical solution temperature behaviour.

The dynamic mechanical behaviour (DMTA) of both blends and solutions was determined using a Polymer Laboratories MkII. The measurements were performed in a double cantilever bending mode using a frequency of 1 Hz and heating rate of  $2^\circ\text{C min}^{-1}$ . The maximum of the loss peak,  $\tan \delta$ , was taken as the glass transition temperature,  $T_g$ .

A Rheometrics RDSII spectrometer operated at a frequency of  $10 \text{ rad s}^{-1}$  was used to measure the viscosity of the PPE–PS/epoxy solutions, by cooling ( $5^\circ\text{C min}^{-1}$ ) homogeneous samples from a starting temperature of  $225^\circ\text{C}$ .

### 2.3. Morphology

Scanning electron microscopy (SEM) (Cambridge Stereoscan 200) was used to visualize the morphology. Sample preparations occurred by cryogenic fracture of the PPE–PS/epoxy blends. Additionally, for blends possessing a sub-micron morphology, transmission electron microscopy (TEM) (Jeol TEM 2000 FX) was performed. Samples were ultramicrotomed (Reichert Ultracut E) at room temperature and, subsequently, vapour stained using ruthenium tetroxide ( $\text{RuO}_4$ ).

If possible, an even better estimate of the epoxy particle size in the blends was obtained by extracting the particles from the PPE–PS matrix. An ultracentrifuge was used to separate the non-soluble thermosetting epoxy particles from the soluble PPE–PS matrix. After each of the three ultracentrifuge steps, the solvent was replaced. Chloroform was used in the first step, toluene during the remaining two steps. An aluminum strip was immersed in the final solution and, subsequently, dried at  $100^\circ\text{C}$  for 20 h, before studying the particles size by using SEM.

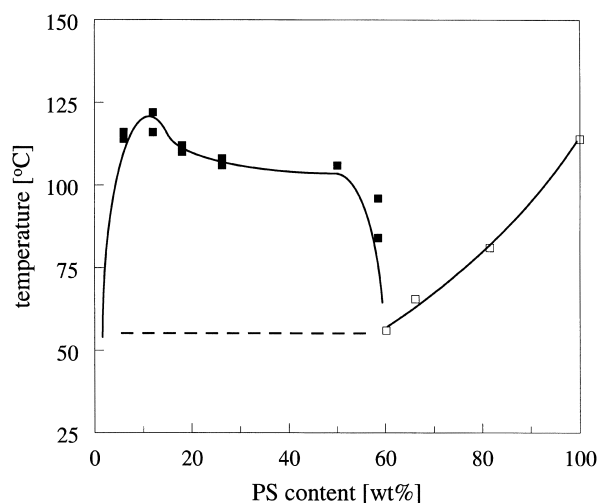


Fig. 1. Binary phase diagram of PS/epoxy: (■) cloud point data; (□) glass transition temperatures; (---)  $T_g$  of the phase separated solutions.

### 3. Results and discussion

#### 3.1. Phase behaviour of binary epoxy solutions

First the phase behaviour of both the binary PS/epoxy and the ternary PPE–PS/epoxy system will be presented and discussed. PPE–PS is known as one of the few combinations of polymers that are miscible over the whole composition range [20,21]. The phase behaviour of PPE/epoxy has been reported earlier by Venderbosch et al. [1] for three PPE molecular weights. The cloud point and vitrification curve of the PS/epoxy system, determined by respectively light scattering and DMTA, are presented in Fig. 1. Solutions with a PS content not exceeding 60 wt% are homogeneous at elevated temperatures but phase separate upon cooling. The curve of the cloud point temperatures shows a rather unexpected concentration independent behaviour in the composition range of 20–50 wt% PS. The maximum

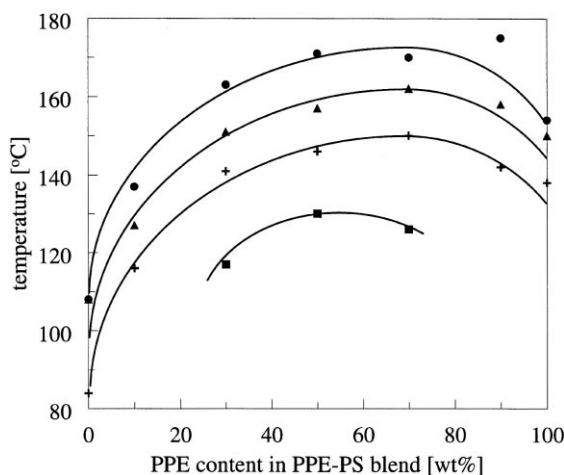


Fig. 2. Cloud point curves of some ternary PPE–PS/epoxy solutions for four fixed epoxy concentrations: (■) 30 wt%, (+) 40 wt%, (▲) 50 wt%, (●) 60 wt%.

cloud point temperature is measured at approximately 125°C, which is low compared to the 180°C found for PPE/epoxy [1]. Upon cooling solutions containing more than 60 wt% polystyrene, vitrification occurs prior to thermally induced phase separation. Visually, homogeneous solidified solutions are obtained, possessing a  $T_g$  in accordance with the Fox relationship [22]. The intersection point of this vitrification curve and the cloud point curve is called the Berghmans point [23] and is found at approximately 60 wt% polymer for both PS/epoxy and PPE/epoxy. To a good approximation, the phase separated solutions containing 60 wt% epoxy or less will all possess a  $T_g$  equal to that of the Berghmans point, as is represented by the dashed line.

#### 3.2. Phase behaviour of ternary PPE–PS/epoxy solutions

The phase behaviour of ternary PPE–PS/epoxy solutions has been studied. In Fig. 2 the cloud point temperatures of four solutions with varying PPE–PS ratios are presented at constant epoxy concentrations of respectively 30, 40, 50 and 60 wt%. Cloud point curves are found over the whole PPE–PS composition range at epoxy concentrations of 60, 50 and 40 wt%, indicating that thermally induced phase separation occurs prior to vitrification. Higher temperatures are required to obtain homogeneous solutions when the epoxy concentration in the ternary system is increased. Moreover, the cloud point temperatures for the PS rich solutions (left-hand side in the phase diagram) are lower compared to those for the PPE rich solutions (right-hand side). In the 30 wt% epoxy solutions, thermally induced phase separation occurs only if both PPE and PS are present in considerable amounts, while the binary solutions, PPE/epoxy and PS/epoxy, vitrify prior to demixing. The miscibility over the whole PPE–PS composition range is retained up to an epoxy concentration of 20 wt%. The measured cloud points are used to construct a ternary cloud point diagram as presented in Fig. 3. The baseline of the diagram represents the homogeneous PPE–PS blend while the two remaining axes cover the cloud point curves of the PS/epoxy system (see Fig. 1) and the PPE/epoxy system (see Ref. [4]). The collection of Berghmans points is represented by the dashed line (B.P., the Berghmans curve). PPE and/or PS rich solutions possessing compositions underneath this line will all vitrify upon cooling and, therefore, remain homogeneous. In contrast, if the epoxy concentration exceeds those given by the Berghmans curve, phase separation will occur upon cooling. The epoxy concentration at the Berghmans points appears to increase from approximately 60 wt% for the binary systems, PS/epoxy and PPE/epoxy, to almost 80 wt% for a PPE–PS 50–50 blend. The cloud point data presented in Fig. 2 are used to construct the four isothermal cloud point curves for 120, 140, 150 and 160°C in Fig. 3. A rather similar concentration dependence is observed to that for the Berghmans curve. The strong curved shape of the isotherms as the PS/epoxy axis is approached is the result of

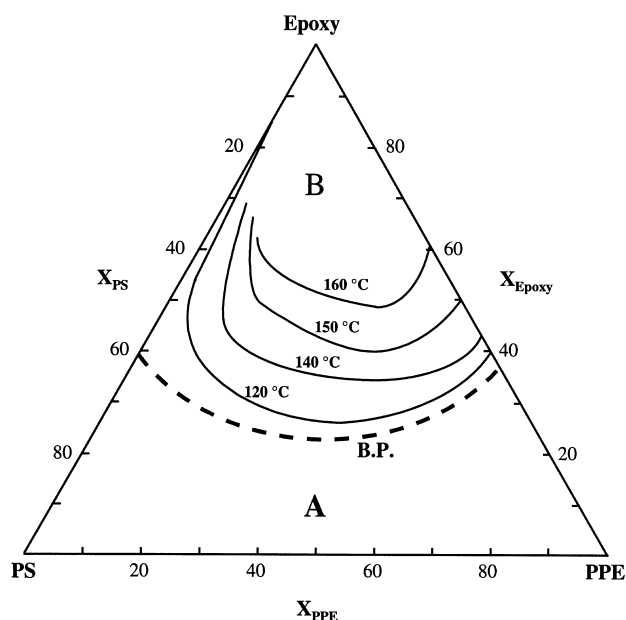


Fig. 3. Ternary cloud point diagram of the ternary PPE–PS/epoxy solution. The lines drawn represent the isothermals of measured cloud points at the indicated temperatures. – – (B.P.) represents the collection of Berghmans points which separates: (A) direct vitrification from homogeneous solution and (B) thermally induced phase separation prior to vitrification.

the concentration independent cloud point temperatures as observed for the binary PS/epoxy system (see Fig. 1).

### 3.3. Curing of PPE–PS/epoxy solutions

In order to cure the epoxy resin, a curing agent has to be added to PPE–PS/epoxy solutions. Since this changes the ternary solution into a quaternary system, the phase behaviour as presented in Fig. 3 can only be used as a first indication for the miscibility at a certain composition. Most probably, the curing agents applied in this study do not decrease the compatibility since an improved miscibility has been reported once a curing agent such as M-CDEA is introduced to PPE/epoxy [24,25].

Upon curing of the homogeneous solutions, chemically induced phase separation is expected to occur since the epoxy resin is transformed into a non-solvent. In the case of PPE/epoxy, the concomitant phase inversion leads to a final morphology consisting of dispersed epoxy particles in a PPE matrix as can be observed in Fig. 4(a). The epoxy spheres appear to be partially covered with PPE. A similar morphology is obtained upon curing a PS/epoxy solution; however, as can be observed in Fig. 4(g), the epoxy particles appear to be much smoother. Fig. 4 shows that the amount of matrix covering the epoxy particles gradually changes with the PPE–PS ratio which is, most probably, the result of the reactivity of the PPE component. The hydroxyl end-groups of the PPE polymer can react with the epoxy resin, giving rise to an improved interfacial bonding compared to PS/epoxy. The formation of this ‘co-polymer’ will most

probably also act as compatibiliser and, therefore, will somewhat reduce the final epoxy particle size in the blend. This is confirmed by the particles sizes depicted from Fig. 4, which decrease from approximately 3  $\mu\text{m}$  for PS/epoxy to 2  $\mu\text{m}$  for PPE/epoxy.

In the case of curing the binary solution, PPE/epoxy and PS/epoxy, a two phase system is obtained. In the present case of a ternary system where, besides epoxy as the reactive solvent, both PS and PPE are present, a two phase system also apparently results (see Fig. 4). More direct evidence than from SEM micrographs can, however, only be obtained from monitoring the glass transition temperatures of the resulting blends by using dynamic mechanical analysis. The results are presented in Fig. 5 which shows the  $T_g$  values of the PPE–PS phase in the cured systems compared to those of neat PPE–PS blends. The  $T_g$  of the cured blends follows the trend of the pure PPE–PS, confirming that a two phase system results, which roughly follows the Fox equation [21]. Some care in the interpretation of these results is, however, necessary since the  $T_g$  of the epoxy phase formed is found in the same range as the intermediate PPE–PS blend compositions. The absence of separate PPE and/or PS transitions confirms, however, that the PPE–PS phase can be considered as one single phase during chemically induced phase separation in the ternary solutions.

### 3.4. Influence of curing temperature on the morphology

#### 3.4.1. One-step curing at $T_g$

Mechanical properties of blends are determined by the properties of the constituent phases and by their morphology. Venderbosch et al. [1,3] did not observe any relevant changes in morphology of PPE/epoxy systems upon varying the curing temperature, the curing agent and its amount over a relatively broad range. Nevertheless, it could be expected that extreme curing conditions should yield different results. As an example, Fig. 6(b) and 6(c) show the resulting morphology of PPE/epoxy (70/30) cured at a very low curing temperature of 105°C, which is indeed considerably lower than the temperature range used by Venderbosch et al. (see Fig. 6(a)). The size of the epoxy particles is decreased by one order of magnitude, from approximately 1.5  $\mu\text{m}$  to 200 nm (compare Fig. 6(a) and 6(b)). This substantial difference in the resulting particle size can be attributed to the large influence of the curing temperature on the coalescence rate versus reaction rate [7,9,14]. The final morphology size in processes involving chemically induced phase separation (CIPS) will depend on the rate of coarsening after phase separation and the available time which is determined by gelation or vitrification of the epoxy phase. Hence, at high reaction rates, gelation and, consequently, morphology fixation occurs at an early stage of the coarsening process [17], while on the contrary a low curing temperature yields a high viscosity that slows down the coalescence rate. The lower limit of the second route is, obviously, curing at the  $T_g$  of the initial solution. This was already partially recognised by

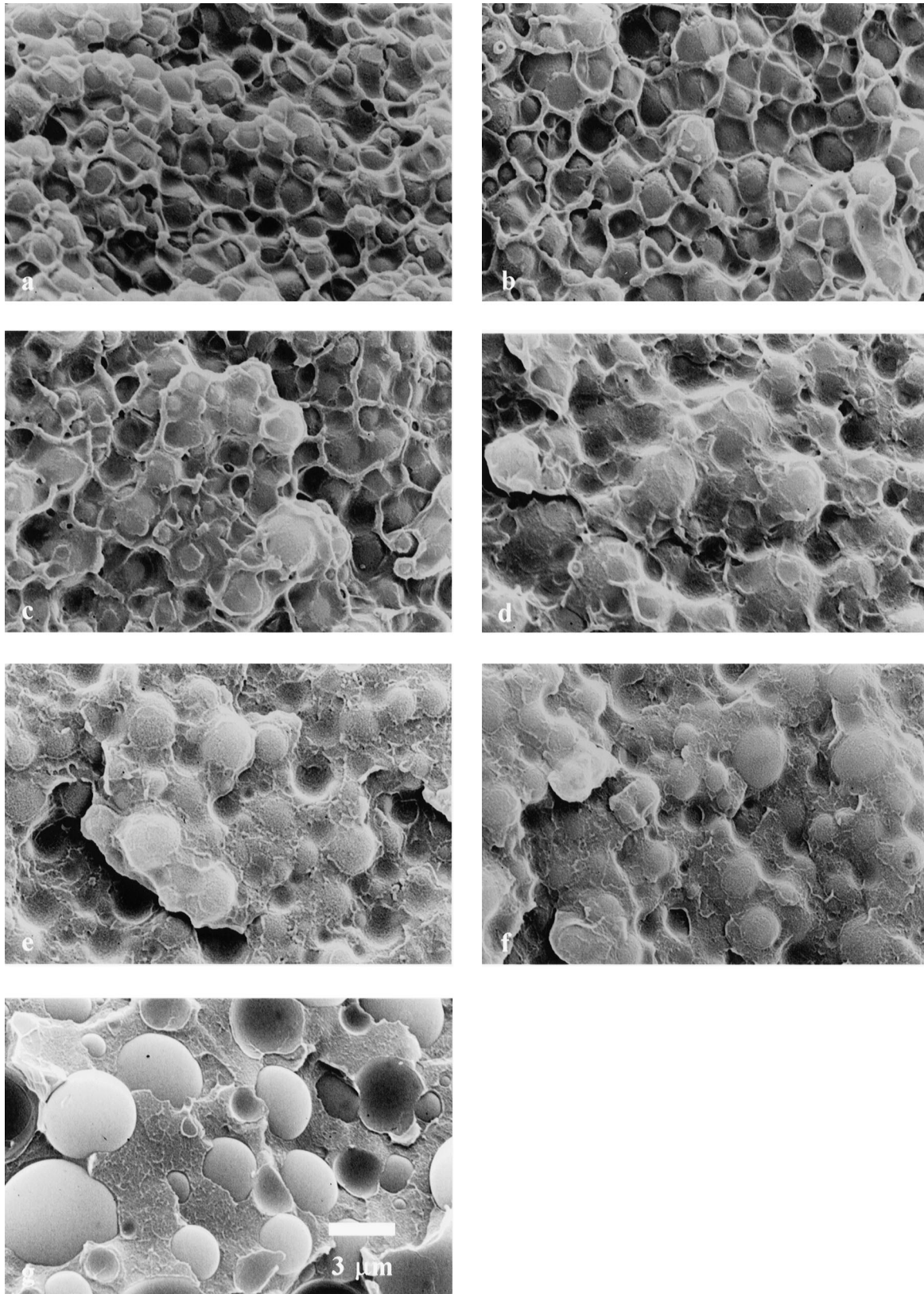


Fig. 4. Morphology of PPE-PS/epoxy blends containing 50 wt% epoxy, cured at 225°C (M-CDEA). PPE-PS: (a) 100–0, (b) 90–10, (c) 70–30, (d) 50–50, (e) 30–70, (f) 10–90, (g) 0–100.

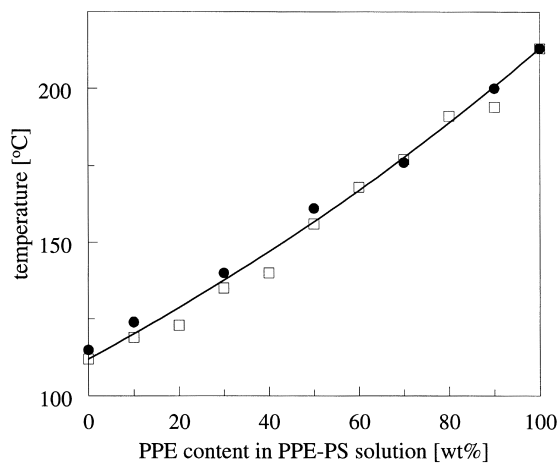


Fig. 5. Glass transition temperatures of the PPE–PS phase in binary blends (□) and in the PPE–PS/epoxy blends (●).

Yamanaka and Inoue [9]. A clear disadvantage of curing at  $T_g$  is that curing cycles will be long (in the order of hours). This is because the solution preparation requires high temperatures (see the phase diagram in Fig. 3). Consequently, low reactive curing agents must be used or, alternatively, extremely short mixing times.

Moreover, the  $T_g$ -curing approach can only be applied for systems which remain homogeneous and can, therefore, only successfully be performed for PPE–PS/epoxy solutions that vitrify upon cooling. For example, for solutions

with 30 wt% epoxy, this can be realized as long as either the PPE or the PS content is high (e.g. PPE–PS/epoxy 90–10/30 or 10–90/30) (see Fig. 7(a) and Fig. 9 for 90–10/30). In systems where both PPE and PS are present in considerable amounts, e.g. 50–50/30 in Fig. 7(b), a micron sized morphology always resulted rather than the 200 nm sized dispersions found earlier. The morphology of this blend (Fig. 7(b)) is the result of thermally induced phase separation prior to curing, which occurs upon cooling to the  $T_g$ , i.e. 90°C (which would have been the solution  $T_g$  if thermally induced phase separation had not occurred). The particle size obtained is only slightly smaller compared to the same system cured at 225°C, for which the morphology is the result of chemically induced phase separation only.

Thus far, all examples presented on morphology control by adapting the curing schedule were taken from systems with a relatively low epoxy fraction. The reason for this is the requirement of obtaining an initially vitrified solution, which is, for the PPE–PS system, only possible for a solvent content of 30 wt% or less (see Fig. 3). The general applicability of the new processing route described here is confirmed by polyetherimide (PEI) epoxy for which vitrified solutions can be obtained up to an epoxy content of 70 wt% [5]. In Fig. 8, two final morphologies of a 50/50 solution are presented which are the result of curing at the  $T_g$  of the initial solution (90°C) and at a high temperature (225°C), respectively. This example clearly illustrates the previous conclusion that morphology development can be controlled

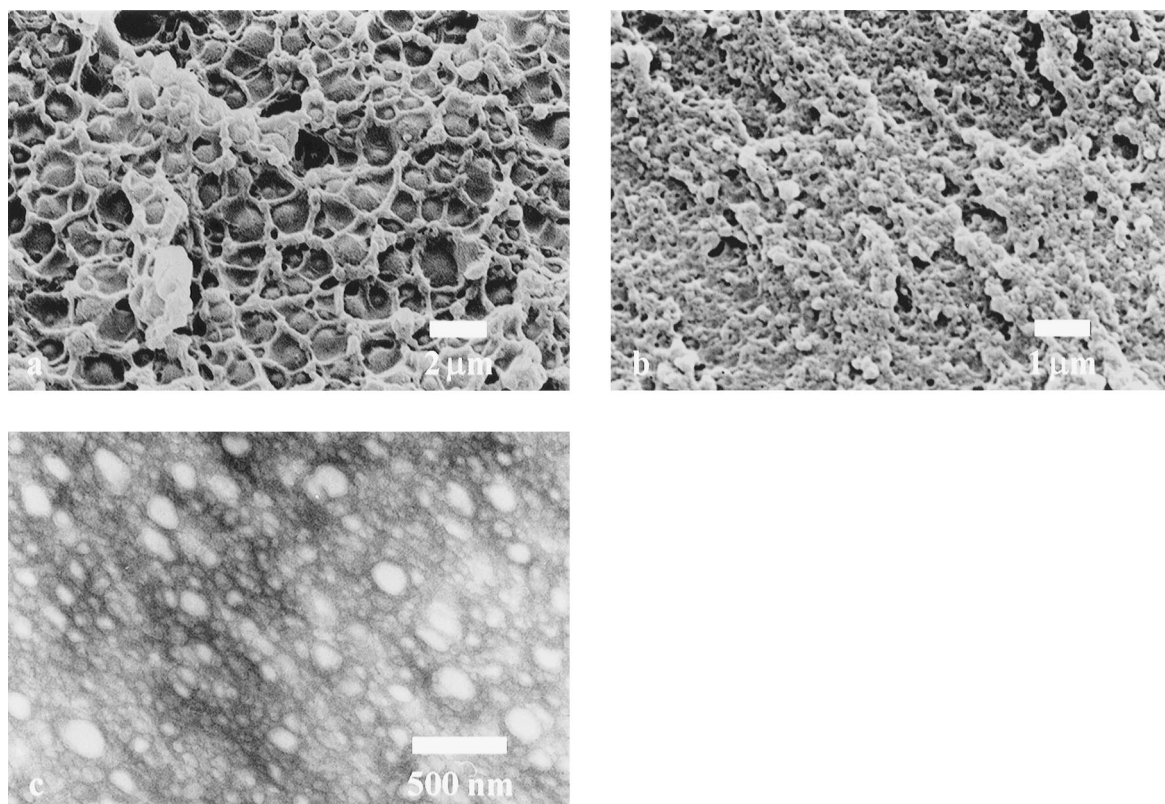


Fig. 6. Morphology of PPE/epoxy 70/30 blends: (a) SEM,  $T_{\text{cure}} = 225^\circ\text{C}$ ; (b) SEM,  $T_{\text{cure}} = 105^\circ\text{C}$ ; (c) TEM,  $T_{\text{cure}} = 105^\circ\text{C}$ .

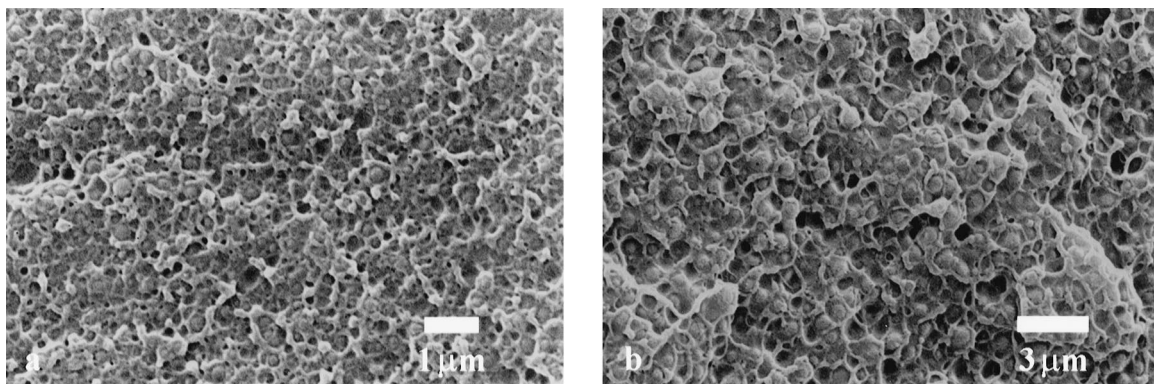


Fig. 7. SEM micrographs of PPE–PS/epoxy blends: (a) 90–10/30,  $T_{\text{cure}} = 105^{\circ}\text{C}$ ; (b) 50–50/30,  $T_{\text{cure}} = 90^{\circ}\text{C}$ .

by affecting the coarsening process after phase separation and that this procedure is not restricted to systems with relatively low solvent contents.

#### 3.4.2. Multi-step curing at $T_g$

Another drawback of curing at relatively low temperatures is that no full epoxy conversion and phase separation can be obtained as a result of vitrification of either the epoxy rich or the PPE–PS rich phase. This causes a contradiction in the curing schedule; a low curing temperature is desired to obtain the sub-micron morphologies while higher curing temperatures are needed to reach full conversion. Therefore, a stepwise curing procedure is required to obtain maximum conversion meanwhile maintaining the  $T_{\text{cure}}(t) = T_g(t)$  condition to control the morphology. Ultimately, this is realised by increasing the curing temperature exactly as the  $T_g$  of the system is increased by the proceeding reaction and phase separation.

The morphology of a PPE–PS/epoxy 90–10/30 blend cured at the  $T_g$  of the initial solution ( $105^{\circ}\text{C}$ ) is shown in Fig. 9(a). For comparison, Fig. 9(b) shows that of the same system, also cured at  $T_g$ , but subsequently post-cured at 150, 180 and  $200^{\circ}\text{C}$ . Obviously, the particles size did not increase during post-curing. In Fig. 10, the dynamic mechanical behaviour of these blends before and after curing and post-curing is depicted. Although the morphology

is fixed after the first curing step at  $105^{\circ}\text{C}$ , the DMTA results clearly show a continuing reaction with increasing curing temperature. Even though the exact interpretation of these DMTA data is somewhat obscured by the ongoing reaction during the measurements (especially at the lower conversions, lines i and ii), some useful information is still obtained. As observed in Fig. 10(a), the modulus of the uncured system (curve a) falls at a significantly lower temperature than for the cured systems (curves ii, iii, iv and v). Post-curing clearly shifts the  $T_g$  of the system to higher temperatures, from approximately  $140^{\circ}\text{C}$  after the first curing step, to almost  $200^{\circ}\text{C}$  (see also the  $\tan \delta$  measurements in Fig. 10(b)). As the curing temperature approaches  $200^{\circ}\text{C}$  (curves iii, iv and v), the maximum in  $\tan \delta$  can indeed be related to the  $T_g$  values of the blend. Two phases are distinguished: an epoxy-rich phase with a  $T_g$  of  $\sim 160^{\circ}\text{C}$  and a PPE–PS rich phase with a  $T_g$  of  $\sim 190^{\circ}\text{C}$ . Only a minor increase in the  $T_g$  of the latter phase is observed as a result of additional post-curing at 180 and  $200^{\circ}\text{C}$  (curves iv and v). Remarkably, the peaks broaden and partially join, which eventually results, for the epoxy peak, in a shoulder of the PPE–PS transition. These phenomena are known from the formation of interpenetrating polymer network structures in which peak broadening and shifts are ascribed to incomplete demixing or interphase mixing of the crosslinked components [12].

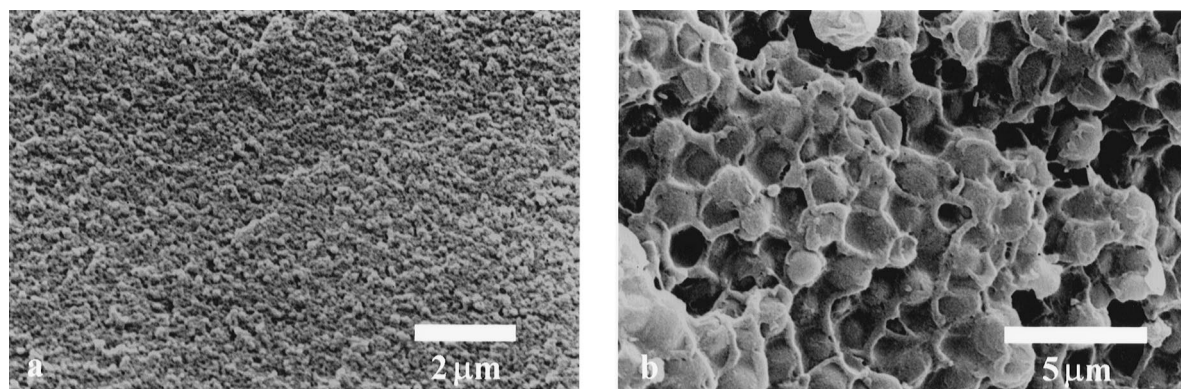


Fig. 8. Morphology of PEI/epoxy 50/50 blend cured at (a)  $90^{\circ}\text{C}$  and (b)  $225^{\circ}\text{C}$ .



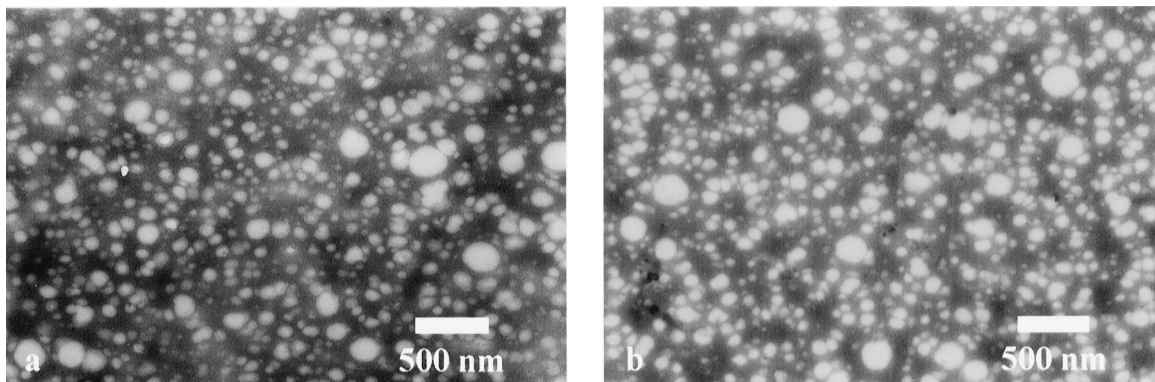


Fig. 9. TEM of PPE-PS/epoxy 90-10/30 cured at: (a) 105°C; (b) cured at 105°C, initially post-cured at 150°C and, subsequently, at 180 and 200°C.

### 3.5. Influence of viscosity on the morphology

Generally, it will be difficult to independently study the influence of the viscosity and reaction rate on the resulting morphology. This is caused by the fact that both parameters are a function of temperature and, therefore, cannot be

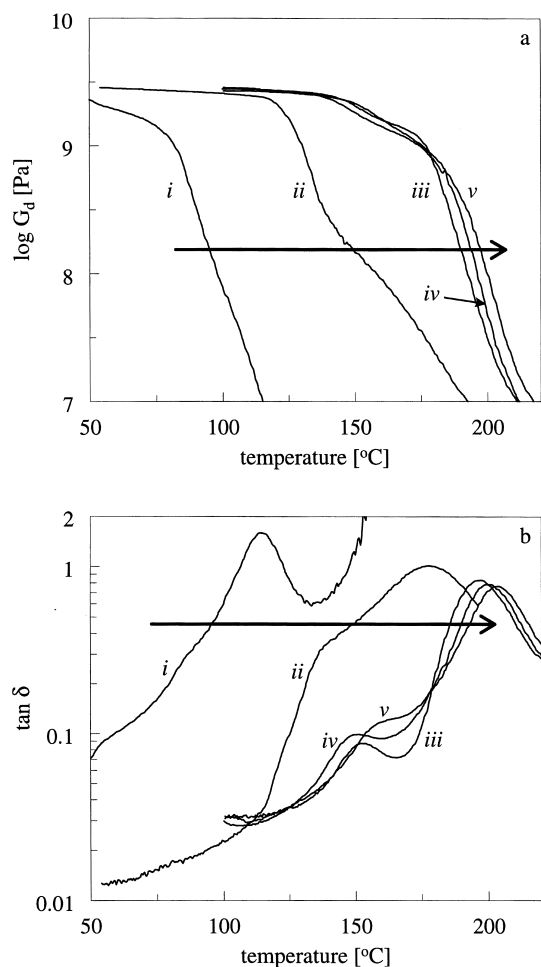


Fig. 10. Dynamic modulus ( $G_d$ ) (a) and a loss angle ( $\tan \delta$ ) (b) versus temperature, of a PPE-PS/epoxy 90-10/30 solution prior to curing (i), after the first curing step at 105°C (ii), and after the additional post-curing steps at 150°C (iii), 180°C (iv), 200°C (v).

varied independently. However, the PPE-PE system offers the unique possibility to study the influence of the viscosity at a fixed curing temperature by varying the  $T_g$  of the initial solution via changing the PPE-PS ratio. One has to keep in mind, however, that the overall reaction rate always consists of a chemical reaction rate combined with a diffusion rate [26]. The reaction rate does not change during curing at a fixed temperature while the diffusion rate still does, given its dependence on the viscosity and thus on the PPE-PS ratio. However, this last effect could be of minor importance, considering all complex processes involved during chemically induced phase separation.

A 20 wt% epoxy system is chosen, since higher solvent concentrations result in a thermally induced phase separation as explained (Fig. 3). The curing temperature is chosen equal to the  $T_g$  of a PPE-PS/epoxy 50-50/20 solution (i.e. approximately 90°C). Consequently, systems with more than 50 wt% PPE (relative to PS) are initially cured below their  $T_g$ , and those with less than 50 wt% PPE are cured above their  $T_g$ . The morphology of the blends is visualised by using TEM (see Fig. 11). For the sample with the highest amount of PS (PPE-PS 10-90), a rather coarse morphology is observed (see Fig. 11(a)). The difference between  $T_g$  of the initial solution and the curing temperature is apparently too large. Upon increasing the PPE content, from PPE-PS 10-90 to 30-70, the particle size decreases, as expected (see Fig. 11(b)). This difference is ascribed to the enhanced viscosity, preventing coalescence. Fig. 12 shows this more clearly for the extracted epoxy particles of PPE-PS/epoxy 30-70/30 after curing at an elevated temperature of 225°C (Fig. 12(a)) and close to the initial  $T_g$  of the solution (90°C, Fig. 12(b)). Upon increasing the PPE content, no further decrease in particle size is found (see Fig. 11(c)). Remarkably, however, is the fact that the blend obtained can no longer be dissolved but only swells upon addition of solvent, which suggests the formation of a phase inverted or bicontinuous morphology or, alternatively, a semi-interpenetrating polymer network [12,13]. This trend is confirmed by the samples possessing the highest PPE contents (PPE-PS 70-30 and 90-10) that also cannot be dissolved. They are cured below the  $T_g$  of the initial solution which appears to prevent



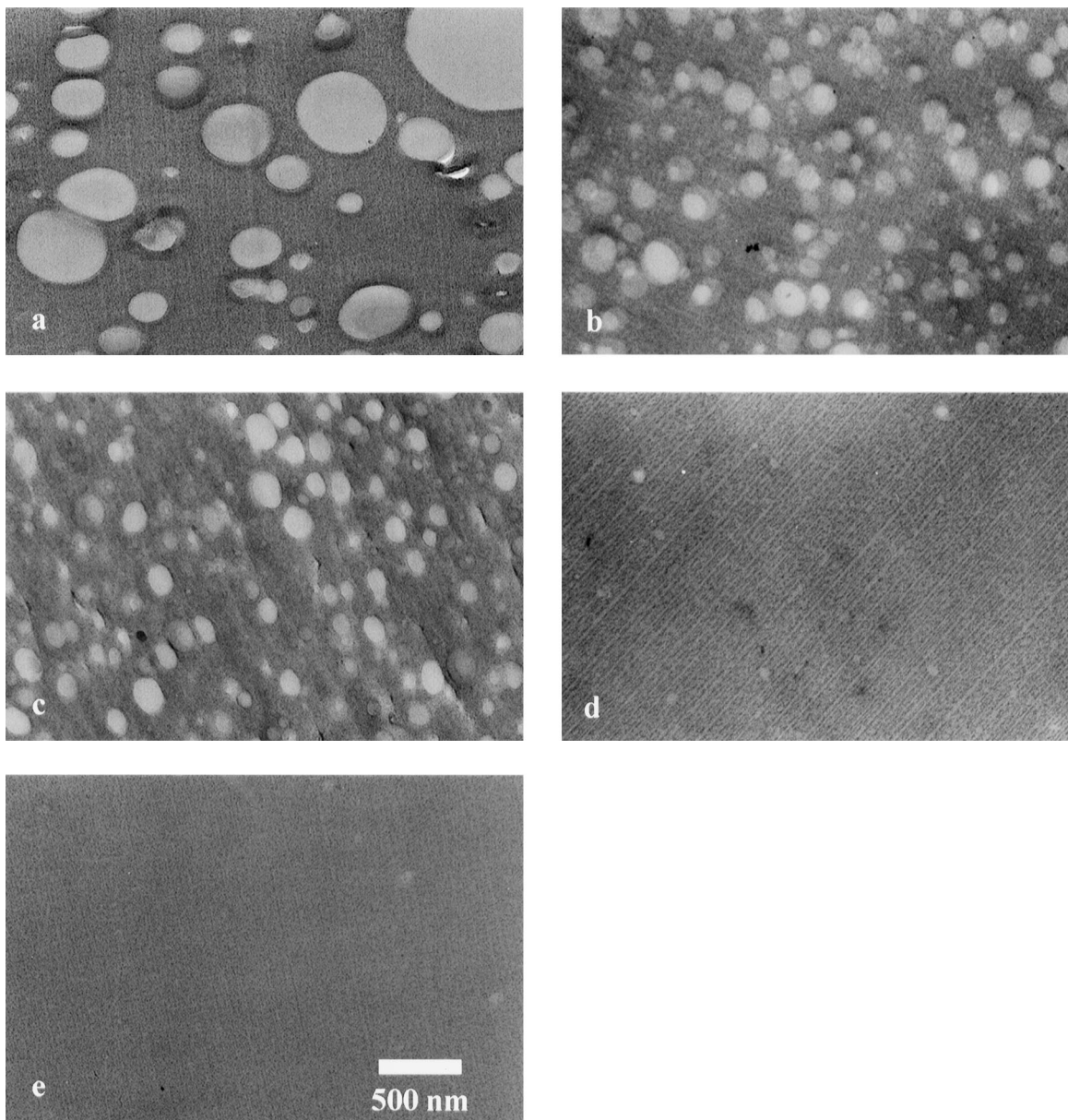


Fig. 11. TEM of PPE–PS/epoxy blends cured at 90°C: (a) 10–90/20, (b) 30–70/20, (c) 50–50/20, (d) 70–30/20, (e) 90–10/20.

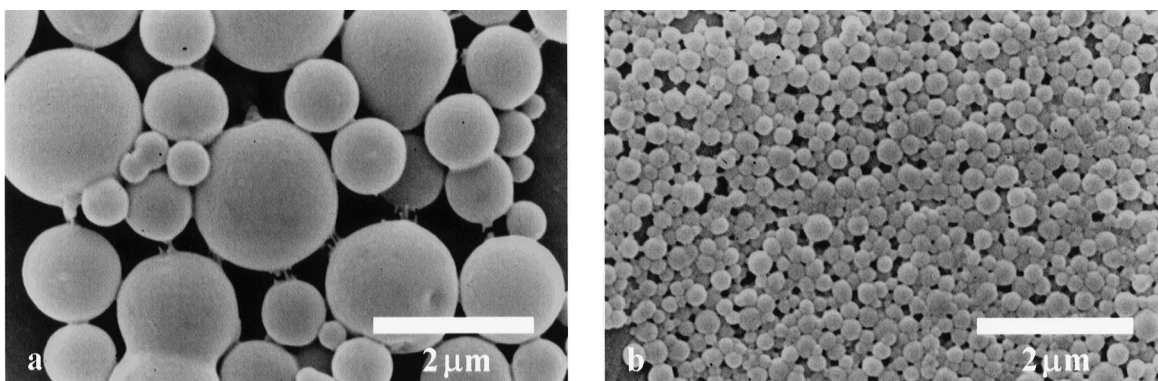


Fig. 12. SEM micrographs of extracted epoxy particles of PPE–PS/epoxy 30–70/30 blends cured at (a) 225°C and (b) 90°C.

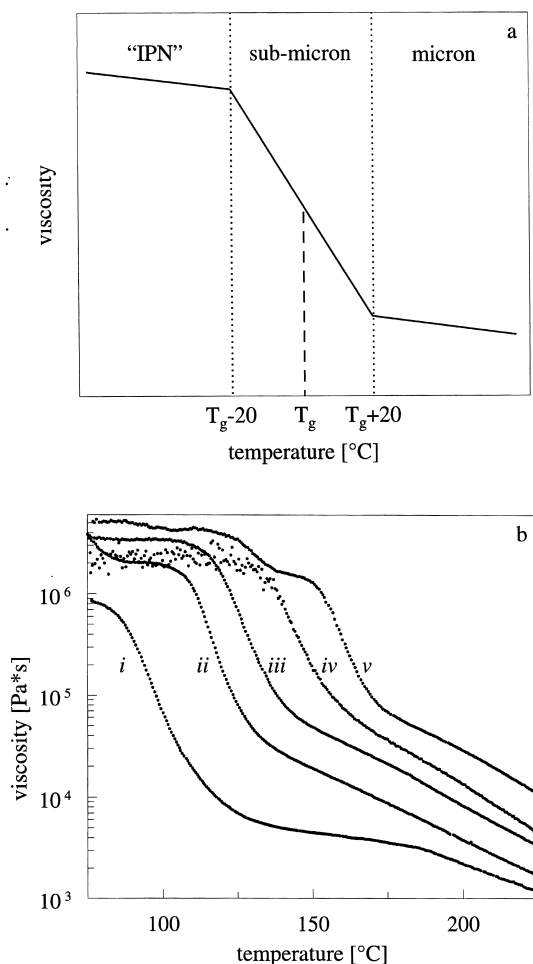


Fig. 13. (a) Schematic representation of the morphology sizes obtained after curing at different temperatures. (b) Viscosity versus temperature for PPE-PS/epoxy solution with 20 wt% (no curing agent) for five PPE-PS ratios: (i) 10–90, (ii) 30–70, (iii) 50–50, (iv) 70–30, (v) 90–10.

the development of a real particle morphology (see Fig. 11(d) and 11(e)).

In conclusion, roughly three types of morphology can be distinguished, as schematically presented in Fig. 13(a), related to the viscosity of the system or the curing temperature. Curing above the  $T_g$  of the initial solution yields micron-sized epoxy particles which are one order larger compared to the sub-micron sized particles for solutions cured around  $T_g$ . From Fig. 13(b) it is concluded that the sub-micron morphology can only be obtained within a temperature window of approximately 40°C. Curing at temperatures lower than  $T_g$ , thus in an almost vitrified system, results in an interpenetrating network where almost no dispersed phase is formed. Curing at higher temperatures yields the well-known micron-sized dispersions. This set of experiments, clearly shows that the current viscosity during curing is the morphology determining parameter.

Of course, the problem of the viscosity dependent diffusion and its influence on the reaction rate remains. However, our statement that this effect is negligible for the systems

studied, is confirmed by the conclusion that for a decreasing reaction rate, the time for the morphology to coarsen after phase separation increases while the final morphology size only decreases upon lowering the curing temperature. Apparently, the increase in viscosity overrules the influence of the reaction rate.

#### 4. Conclusions

The aim of this paper was to study the morphology of blends resulting from chemically induced phase separation processes. We attempted to independently vary the different influences on the processes involved. Therefore, the system PPE-PS/epoxy was studied allowing for an independent change of viscosity and curing temperature. Initially, the phase behaviour of binary PS/epoxy and ternary PPE-PS/epoxy systems was studied. Thermally induced phase separation upon cooling occurs for solutions with 30 wt% epoxy or more while those with a relatively low epoxy content are compatible over the whole PPE-PS composition range. This compatibility of the ternary PPE-PS/epoxy blend is less compared to both binary PPE/epoxy and PS/epoxy systems, reflected by the higher cloud point temperatures.

Upon curing of PPE-PS/epoxy solutions, phase separation occurs which results in a two phase morphology consisting of dispersed epoxy particles in a PPE-PS matrix.

An extremely fine, sub-micron, morphology can be obtained by controlling the morphology coarsening process after phase separation. For solutions that vitrify upon cooling prior to the occurrence of thermally induced phase separation, this can be achieved by applying a protocol of curing at the glass transition temperature of the initial solution. In this case, phase separation occurs in a highly viscous medium which restricts the coarsening process and, in the end, results in a sub-micron morphology. This morphology can be sustained during additional post-curing steps, necessary to reach a maximum conversion of the epoxy.

By changing the PPE-PS ratio, the PPE-PS/epoxy system offers the unique possibility to vary the viscosity independently of the curing temperature. Generally, three types of morphologies are identified. If the PS content in the initial solution is high (e.g. PPE-PS/epoxy 10–90/20), a micron-sized morphology is obtained. In contrast, a real sub-micron morphology is obtained as the PPE content is increased (PPE-PS/epoxy 30–70/20, 50–50/20). This remarkable decrease in the size of the dispersed phase can only be explained in terms of the increasing viscosity, when the PPE content is increased, restricting the morphology to coarsen after phase separation. As the PPE content is increased even further (PPE-PS/epoxy 70–30/20, 90–10/20), TEM no longer shows any evidence of a second phase and those blends can no longer be dissolved. This either indicates the formation of a semi-interpenetrating polymer network or the occurrence of a (partial) phase inversion.

## Acknowledgements

The authors would like to thank E. Grimminck, C. Widdershoven and C. van Zantvoort for performing most of the experimental work.

## References

- [1] Venderbosch RW, Meijer HEH, Lemstra PJ. *Polymer* 1994;33(20):4349.
- [2] Venderbosch RW, Meijer HEH, Lemstra PJ. *Polymer* 1995;36(6):1167.
- [3] Venderbosch RW, Meijer HEH, Lemstra PJ. *Polymer* 1995;36(15):2903.
- [4] Gomez CM, Bucknall CB. *Polymer* 1993;34(10):2111.
- [5] Park JW, Kim SC. *IPNs around the world*. Chichester: Wiley, 1997:27.
- [6] Chean CS, Eamor MW. *Polymer* 1995;36(15):2883.
- [7] Min BG, Hodgkin JH, Stachurski ZH. *J Appl Polym Sci* 1993;50:106.
- [8] Akay M, Cracknell JG. *J Appl Polym Sci* 1994;52:663.
- [9] Yamanaka K, Inoue T. *Polymer* 1989;30:662.
- [10] Janssen JMH, Meijer HEH. *Polym Eng Sci* 1995;35:1766.
- [11] Bucknall CB. *Toughened plastics*. London: Applied Science, 1977.
- [12] Klemperer D, Sperling LH, Ultracki LA. *Interpenetrating polymer networks*. Advanced Chemistry Series. Washington, DC: ACS, 1994.
- [13] Kim SC, Sperling LH. *IPNs around the world*. Chichester: Wiley, 1997.
- [14] Inoue T. *Prog Polym Sci* 1995;20:119.
- [15] Brown JM, Srinivasan S, Rau A, Ward TC, McGrath JE, Loos AC, Hood D, Kranbeuhl DE. *Polymer* 1996;37(9):1691.
- [16] Kim SC, Ko MB, Won HJ. *Polymer* 1995;36(11):2189.
- [17] Yamanaka K, Takagi Y, Inoue T. *Polymer* 1989;60:1839.
- [18] Verchere D, Pascault JP, Sautereau H, Moschiar SM, Riccardi CC, Williams RJ. *J Appl Polym Sci* 1991;42:701.
- [19] Sanden van der MCM, Meijer HEH, Lemstra PJ. *Polymer* 1993;34(10):2148.
- [20] Gallagher RK. *J Chem Phys* 1964;41:3061.
- [21] Prest WM, Porter RS. *J Polym Sci Phys Ed* 1972;10:1639.
- [22] Fox TG. *Bull Amer Phys Soc* 1956;1:123.
- [23] Vandeweerd P, Berghmans H, Tervoort Y. *Macromolecules* 1991;24:3547.
- [24] Riccardi CC, Borrajo J, Williams RJJ, Girard-Reydet E, Sautereau H, Pascault JP. *J Polym Sci Phys Ed* 1996; to be published.
- [25] Pascault JP. *Macromol Symp* 1995;93:43.
- [26] Girard-Reydet E, Riccardi CC, Sautereau H, Pascault JP. *Macromolecule* 1995;28:7599.